condensed matter

MDPI

Review

Superconductivity in the α-Form Layer Structured Metal Nitride Halide

Masashi Tanaka [1,*], Noriyuki Kataoka [2] and Takayoshi Yokoya [2,3]

[1] Graduate School of Engineering, Kyushu Institute of Technology, Kitakyushu 804-8550, Japan
[2] Graduate School of Natural Science and Technology, Okayama University, Okayama 700-8530, Japan; po5n3yf0@s.okayama-u.ac.jp (N.K.); yokoya@cc.okayama-u.ac.jp (T.Y.)
[3] Research Institute for Interdisciplinary Science (RIIS), Okayama University, Okayama 700-8530, Japan
* Correspondence: mtanaka@mns.kyutech.ac.jp; Tel.: +81-93-884-3204

Abstract: Layered metal nitride halides *M*N*X* (*M* = Ti, Zr, Hf; *X* = Cl, Br, I) have two polymorphs, including α- and β-forms, which have the FeOCl and SmSI structures, respectively. These compounds are band insulators and become metals and show superconductivity after electron doping by intercalating alkali metals between the layers. The superconductivity of β-form had been extensively characterized from decades ago, but it is not easy to consistently interpret all experimental results using conventional phonon-mediated Bardeen–Cooper–Schriefer mechanisms. The titanium compound TiNCl crystallizes only in the α-form structure. TiNCl also exhibits superconductivity as high as ~16 K after electron doping by intercalating metals and/or organic basis. It is important to compare the superconductivity of different *M*–N networks. However, α-form compounds are vulnerable to moisture, unlike β-form ones. The intercalation compounds are even more sensitive to humid air. Thus, there are few experimental studies on the superconducting mechanism of α-form, although it has been discussed for exotic Cooper-pairing mechanisms. This short review gathers the recent progress in experimental studies of TiNCl.

Keywords: α-form layered nitride halides; intercalation; electron doping; superconducting mechanism; photoemission spectroscopy

Citation: Tanaka, M.; Kataoka, N.; Yokoya, T. Superconductivity in the α-Form Layer Structured Metal Nitride Halide. *Condens. Matter* **2022**, *7*, 33. https://doi.org/10.3390/condmat7020033

Academic Editor: Andrea Perali

Received: 7 February 2022
Accepted: 28 February 2022
Published: 1 April 2022

1. Introduction

Transition metal nitride halides *M*N*X* (*M* = Ti, Zr, Hf; *X* = Cl, Br, I) belong to a characteristic class of layered materials that exhibits superconductivity by carrier doping [1–3]. They have two polymorphs, including α- and β-forms, which have the FeOCl and SmSI structures, respectively [4,5]. These compounds are band insulators and can be intercalated with alkali or alkaline earth metals to significantly modify the physical properties without changing their basic crystal structures. Alkali atoms with/without organic molecules are intercalated into the van der Waals gap between two adjacent *X* layers with the realignment of *M*N*X* layers.

The β-form polymorph contains double honeycomb-like *M*N layers sandwiched by halogen layers, as shown in Figure 1a,b. Band-insulating β-HfNCl is electron-doped and becomes metallic through intercalation [2,4]. The compound shows superconductivity at a transition temperature (T_c) above 25.5 K in Li and tetrahydrofuran (THF) cointercalated compound of β-HfNCl [2,4,6]; this family of materials is categorized as high-T_c superconductors. The superconductivity can also be induced by carrier doping with an electronic-double-layer transistor [7–11]. The T_c enhancement has been reported with reducing carrier density [12,13] and the partial substitution *M* site [14]. Electronic structural studies have shown that alkali-metal intercalation adds quasi-two-dimensional electronic states near the Fermi level (E_F), which are hybridized states of Hf 5*d* and N 2*p* orbitals [15–19]. The absence of isotope effect, extremely large superconducting gap value

$2\Delta/k_BT_c$, enhancement of T_c for lower carrier concentration, anomalous doping dependence in anisotropy of superconducting gap, and strong suppression of the coherence peak in nuclear spin-lattice relaxation rate strongly suggest an exotic superconducting state in this material series [13,20–28]. With the extensively characterized superconductivity in β-form *M*N*X*, it is not easy to consistently interpret all experimental results using conventional phonon-mediated Bardeen–Cooper–Schrieffer (BCS) mechanisms [29].

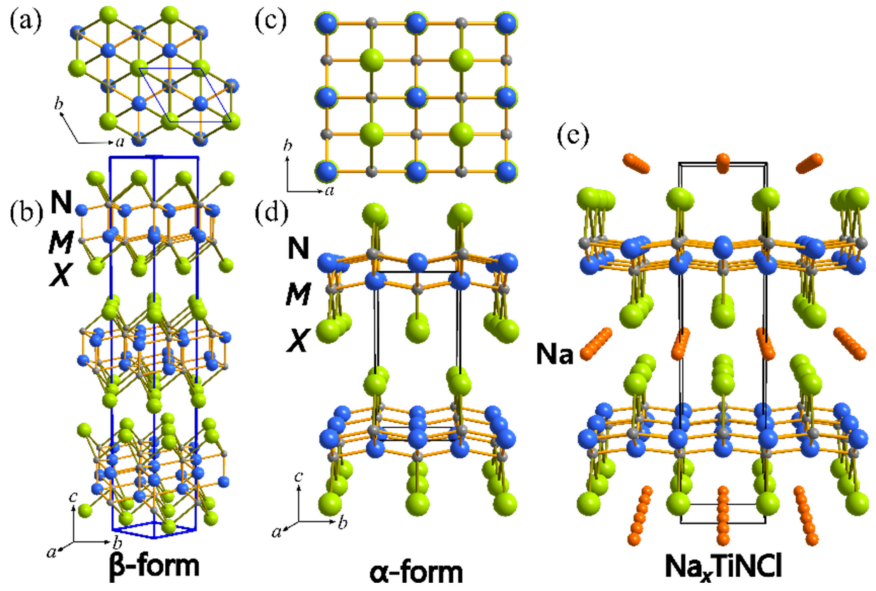

Figure 1. Crystal structure of *M*N*X*: (**a**,**b**) the top and side views of β-*M*N*X*, (**c**,**d**) the top and side views of α-*M*N*X*, respectively, and (**e**) the side view of Na-intercalated TiNCl. Upon the intercalation, TiNCl shows a polytype shift. The lattice type changes from the space group *Pmmn* of the pristine TiNCl to *Bmmb*. Reproduced with permission from Reference [30]. © (2019) The Physical Society of Japan.

The α-form polymorph has an orthogonal *M*N layer network separated by halogen layers, as shown in Figure 1c.d. The titanium compound (TiN*X*) crystallizes only in the α-form structure. TiNCl has been reported to exhibit superconductivity as high as ~16 K after electron doping by intercalating metals and/or organic basis [3,31,32]. The crystal structure of the sodium intercalated TiNCl is also shown in Figure 1e. It is important to compare the superconductivity of different *M*–N networks. However, the α-form polymorphs were considered less good host materials than β-forms. The α-form compounds are vulnerable to moisture, unlike β-form ones; the intercalation compounds are even more sensitive to humid air. Moreover, compared to β-form, they can easily decompose into binary *M*-N compounds, which also shows superconductivity. These facts were also a disadvantage for the physical properties measurements. Therefore, most studies on superconductivity deal with intercalation compounds of the β-forms. In the recent study, the α-*M*N*X* is expected to achieve new applications utilizing two-dimensional nature, such as solar-cell [33], photocatalyst [34,35], energy storage and conversion [36], topological insulator [37–39], electronic devices [40], and optoelectronic devices [41]. However, all these suggestions are based on computational first-principle calculations. Only a few experimental studies of *M*N*X* have been found recently, even if we expand the searching range to β-forms [10,14,42]. The lack of experimental results is somewhat due to the difficulties in synthesizing samples of both the parent and the electron-doped α-forms.

From experimental viewpoints, we have studied the superconductivity of α-form *M*N*X*, TiNCl. This article briefly reviews the preparation and intercalation reactions in TiNCl and its superconductivities. This article will mainly focus on the recent experimental studies on the electronic structure developed in the last decade. The crystal chemistry, the

structural influence of the superconductivity, and the superconductivity of β-form are not included. Reviews of these topics are presented in [4,29,43], and so on.

2. Synthesis and Electron Doping of TiNCl

Juza et al. prepared various pure Ti- and Zr-nitride halides during the 1960s [44–46], and the preparation of TiNCl was firstly reported in 1964 [5]. To understand how it is tricky to handle, let us look back at the synthesizing process in this section.

2.1. Conventional Preparation

For the synthesis of *M*N*X*, the tetrahalides of titanium, zirconium, and hafnium are reacted with ammonia following the generic equation:

$$MX_4 + 4NH_3 \rightarrow MNX + 3NH_4X$$

In the case of *M* = Zr, Hf in the β-form, Yamanaka has efficiently developed the method using a reaction of metal or metal hydride powders with NH_4X [3]. The one-step method in a vacuum-sealed glass tube can also be adopted in a small-scale synthesis of less than ~200 mg [2].

However, in the case of *M* = Ti, especially TiNCl, the easy process cannot be used. In the reaction between Ti and NH_4Cl, TiH_2 is first formed at about 400 °C or lower. Above the temperature at which TiH_2 can be decomposed, TiNCl is not formed, but TiN is formed instead. Then, the ammonia (NH_3) gas should be passed over titanium tetrachloride ($TiCl_4$) in a vertical Pyrex glass reaction cell. The reactant becomes black solid after being self-heated by the heat evolved from the intense exothermic reaction. Due to the high reactivity of $TiCl_4$ with NH_3, the reaction may lead to molecules and complexes of several manners [47]. $TiCl_4$ ammonolysis is energetically favorable [47,48]. $TiCl_4$ forms ammonia-incorporated complexes with the $TiCl_4 \cdot xNH_3$ gross composition, and heating the complexes in ammonia-rich atmosphere results in stepwise amination of $TiCl_4$ to form $TiCl(NH_2)_3$ in the final step [49–51]. The ammonia complexes and aminated $TiCl_4$ were especially the main products at low temperatures below 400 °C [49], while TiN is obtained at higher temperatures. The resulting solids were continuously heated in the same reaction cell at 400 °C for 3–5 h under the ammonia gas stream. Ammonium chloride (NH_4Cl) crystals were grown on the upper part of the reaction cell.

The TiNCl precursor and other related compounds (crude mixture) were formed at the bottom of the glass cell. The by-products necessitate a next purification step. The crude mixture was vacuum-sealed in a Pyrex glass tube with a small amount of NH_4Cl and put into a horizontal furnace with a temperature gradient for one to two weeks. Then, it was purified into highly crystalline TiNCl by chemical transport using NH_4Cl. The end of the glass tube containing the mixture was maintained at 380 °C in the lower temperature zone, and the other end of the glass tube was placed in the higher temperature zone. Purified TiNCl was obtained at the higher temperature zone [52]. TiNCl starts to decompose to TiN at temperatures above 400 °C [53,54]. Once it decomposes into TiN with trivalent titanium, it is hard to return to tetravalent TiNCl. Then, it should be maintained at a temperature as low as possible above 400 °C to obtain impurity-free samples.

Assuming the same reaction as the case of ZrNCl [55], the essential reaction in the chemical vapor transport of TiNCl is expressed as follows:

$$TiCl_4(g) + NH_3(g) \rightarrow TiCl_3(NH_2) + HCl \rightarrow TiNCl(s) + 3HCl(g)\ (>\sim 400\ ^\circ C)$$

Since HCl is not easy to handle in this preparation, it is used as a transport agent by utilizing the dissociation of NH_4Cl into NH_3 and HCl at high temperatures. The actual reaction is then expressed as

$$TiCl_3(NH_2) + NH_4Cl \rightarrow TiNCl(s) + NH_3(g) + HCl(g)$$

After these reactions, we can confirm the purity of the obtained TiNCl by the Rietveld refinement and magnetization measurement with the negligible diamagnetic contribution of TiN below 5 K.

2.2. Preparation Using Sodium Amide

In a study on a superconducting mechanism, the isotope effect on T_c provides crucial evidence of whether electron–phonon interaction is responsible for superconductivity. Considering the above conventional synthesizing process of TiNCl, retaining the ^{15}N isotope using NH_3 gas as a nitrogen source is extremely difficult or almost impossible realistically. However, if the TiNCl precursor could be formed using a solid reagent other than gas NH_3 as a nitrogen source in a closed reaction cell, an essential technique for synthesizing ^{15}N substituents would be developed. It could be led not only to elucidate the superconducting mechanism of TiNCl but also to investigate the isotope effect of other metal nitride superconductors.

$NaNH_2$ is a highly reactive solid nitrogen source used for combustion reaction with 3*d* transition metal chlorides to obtain metal nitrides [56,57]. The reactions are thermodynamically driven by a metathesis reaction involving the formation of stable NaCl. The NaCl does not contribute to chemical transport; if the reaction with $TiCl_4$ can be controlled, TiNCl may be obtained in the sealed glass tube.

When the sealed glass tube containing $TiCl_4$ and $NaNH_2$ was gradually heated up to 150 °C in 12 h and then kept at this temperature for 1-2 days, the infrared spectroscopy, thermogravimetry, and X-ray diffraction measurements of the resulting solids suggested that it contains $TiCl_3(NH_2)$, $TiCl_2(NH_2)_2$, and $TiCl(NH_2)$, together with $TiCl_4 \cdot xNH_3$ [58]. Namely, the reaction at this process can be written as the equation $TiCl_4 + NaNH_2 \rightarrow TiCl_3(NH_2) + NaCl$ in the simplest case. After an important process of removing HCl from the reaction system, we can obtain TiNCl with the whole equation in the simplest case written in $TiCl_4 + NaNH_2 \rightarrow TiCl_3(NH_2) + NaCl \rightarrow TiNCl + NaCl + 2HCl$.

The procedures to obtain TiNCl using $NaNH_2$ can be summarized as the following. (1) The sealed mixture of $TiCl_4$ + $NaNH_2$ is sufficiently reacted around 160 °C to obtain preliminary reacted solids. (2) Open the seal and purge unreacted $TiCl_4$ from the glass tube. Then, evacuate the preliminary reacted solids again with the elevated temperature at 180 °C to remove HCl from $TiCl_3(NH_2)$ and/or other aminated compounds. (3) The heating and evacuation should be stopped before decomposition to TiN occurs and sealed again into a glass tube. (4) The glass tube sends to chemical transport to obtain highly crystalline TiNCl [58].

2.3. Electron Doping by Intercalation

Metal intercalation into TiNCl was developed from an electrochemical process as a cathode material [59]. First, superconducting TiNCl has been achieved by an organic Lewis base pyridine (Py) and alkali metal intercalation [3]. The alkali-metal-intercalated TiNCl was prepared using reactions with alkali metal azides at elevated temperatures of 280–350 °C in a vacuum. The intercalation was carried out in the following manner:

$$TiNCl + (x + y)\, AN_3 > A_yTiNCl_{1-x} + xACl + 3(x + y)/2N_2$$

This reaction was not mild, and partial deintercalation of chlorine atoms occurred simultaneously. The superconducting volume fractions (VF) were as low as 0.1–30%. The samples may have suffered from serious structural damage.

A chemical intercalation method using alkali-metal naphthalene solutions in THF (*A*-Naph/THF; *A* = Li, Na, K, Rb) has been used for β-phase for a long time [60]. This method has dramatically improved the low VF problem [32]. Organic molecules such as THF can be cointercalated into TiNCl at room temperature. The THF-cointercalated phase was changed into uncointercalated compound A_xTiNCl by evacuation. The sample thus obtained showed a shielding VF close to 100% and a clear high onset superconducting transition. By this method, the same α-phase TiNBr has also succeeded in being a superconductor [61]. On

the other hand, α-HfNBr isomorphous with TiNCl did not show superconductivity in the same method. The resistivity was larger than ~10^7 Ω cm; the doped electrons seem to be localized on the reduced Hf sites [62]. It should be noted that only Py intercalated TiNCl showed superconductivity. It appears the combination of guest donors and the amount of doping are important to realize the superconductivity of the α-form *MNX*.

The T_c changes with the basal spacing d along the c axis of the intercalation compound. As shown in Figure 2, the T_c decreases with the increasing d [32]. This fact is in sharp contrast to the observation in β-form, where T_c increases linearly with d in electron-doped ZrNCl and HfNCl [25,63]. The data fit on a linear line with passing through the origin. This fact suggests that the Coulomb interlayer coupling in the pairing mechanism is important in this system [32]. Another study on the α-TiNBr has demonstrated a similar linear relation on the T_c vs. $1/d$ [61]. Harshman et al. reported that the linear dependence is readily explained, giving the interlayer Coulomb interaction model and structure [64]. It is also a future task to experimentally observe the effect of the interlayer interaction on the electronic structure.

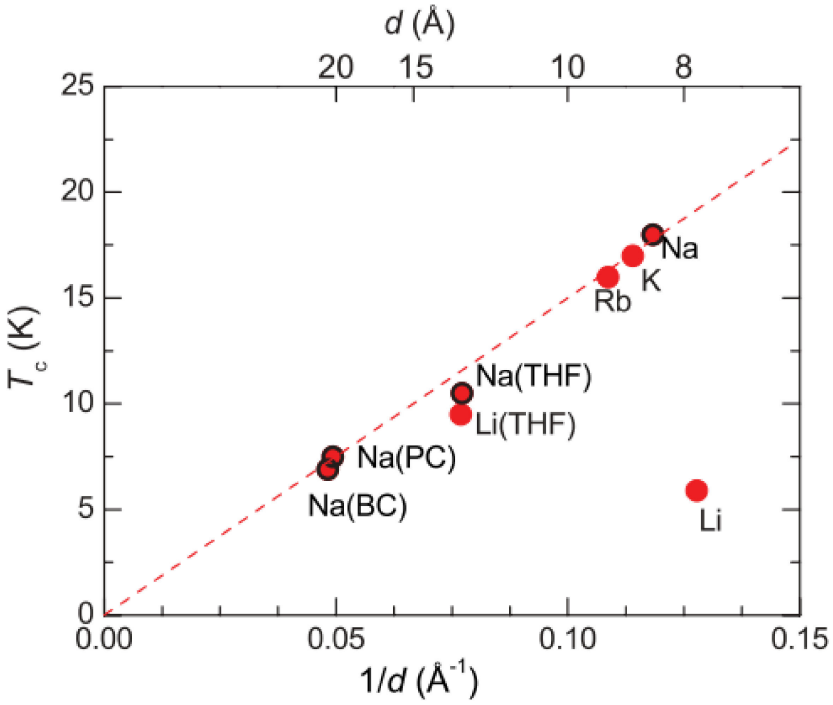

Figure 2. T_c vs. $1/d$ for A_xTiNCl (A = Li, Na, K, Rb) superconductors with and without cointercalation. Reprinted with permission from Ref. [32]. Copyright 2022 American Physical Society.

More recently, it has been found that superconducting properties are also highly dependent on the synthesis temperature of the pristine TiNCl. T_c and volume fraction strongly depend on the higher temperature in the synthesis of the pristine TiNCl. This fact is presumed due to hydrogen incorporation by X-ray diffraction, photoemission spectroscopy, optical spectroscopy, and hydrogen desorption measurements (to be published).

In addition to the above, the mechanism and electronic structure of superconductivity on organic molecules alone without any metal cation are completely unknown. Further experimental studies on intercalated TiNCl are required for a deeper understanding.

3. Electronic Structure of TiNCl

In order to understand the pairing mechanism of this possible exotic superconductor, it is important to clarify how electronic structure evolves with carrier doping. The band structure of pristine TiNCl has been calculated by first-principle calculations [3,65]. It exhibits a two-dimensional feature, with the general flatness of the band along the Γ-

Z direction perpendicular to the layers. The top valence band primarily has a N $2p_x$ character, and the lowest conduction band has a strong Ti $3d_{xy}$ character [65]. There is $3d$ weight in the valence bands and N weight in the conduction bands, respectively, reflecting substantial N $2p$—Ti $3d$ hybridization in addition to the ionic character reflected in their formal charges [65]. The β-form compounds have disconnected cylindrical Fermi surfaces favorable for nesting [66,67], while the electron-doped TiNCl has a single oval Fermi surface centered at the Γ point [65]; the possible nesting between Fermi surfaces discussed for the β-form compounds should be excluded from TiNCl.

Several theoretical ideas are considered in arguing against phonon-mediated superconductivity. Yin et al. discussed the remaining possibilities of spin and charge fluctuations for the high-temperature superconductivity by constructing a many-body extended Hubbard model based on a realistic band structure calculation [65]. They reported that charge fluctuations might play an important role in superconductivity rather than spin fluctuations [65].

On the other hand, Kusakabe showed a criterion for superconductivity by a pair-hopping mechanism for potassium-doped TiNCl [68]. The super-pair hopping process of the spin is possible by providing the connecting orbitals between the two-dimensional electron systems. The locally formed cooper pair in a superconducting layer can be scattered from the neighboring layer via the high-energy intermediate state connecting the layers [68].

However, an electron–phonon mechanism may still be relevant for explaining the high T_c [29]. Yin et al. proposed that the T_c of TiNCl may also be well accounted for the electron–phonon mechanism using hybrid functional instead of local-density approximation (LDA) or generalized-gradient approximation (GGA) functionals in the first principles calculation [69].

In order to verify these theoretical studies, it is important to determine the electronic structure experimentally. A few experimental studies on the superconducting mechanism have been reported up to date. The reduced superconducting gap value $2\Delta/k_BT_c$ has been determined from scanning tunneling microscopy/spectroscopy to be approximately 15 and 12 for K_xTiNCl and Na_xTiNCl, respectively [22,70]. The observed value is four times larger than the mean-field BCS value.

A photoemission spectroscopy (PES) study is the most suitable probe for observations in electronic structure, such as band dispersion. However, angle-resolved photoemission spectroscopy (ARPES) has not been achieved so far for both superconducting α- and β-forms. Although there are several reports of PES for β-form [17–19,71], the electronic structure studies using PES of neither the parent α-form compound nor the doped one have been reported. This problem is mainly due to the difficulty of synthesizing both the parent and the electron-doped α-form samples. However, it would gradually become solved in recent years.

3.1. Micro-PES of Electron-Doped TiNCl

For the first data of the PES study in α-form samples, micro-photoemission spectroscopy (μ-PES) with highly focused synchrotron soft X-ray was performed by Kataoka et al. [30]. In the μ-PES, the angle integrated PES spectra corresponding to the electronic density of states (DOS) of the valence band of TiNCl and Na_xTiNCl were observed, as shown in Figure 3 [30]. The shape of the valence band of TiNCl roughly corresponds to that of band structure calculations. The peaks around 6 eV are hybridized states of Ti $3d$, N $2p$, and Cl $3p$ orbitals, and the 4 eV shoulder structure is dominated by the Cl $3p$ component [30].

The valence band spectrum of Na_xTiNCl exhibits a peak at 6.5 eV, accompanied by an emergence of the metallic state near E_F extending to 1.5 eV. The broad-spectrum has higher binding energy by 0.5 eV than the corresponding band of TiNCl, in line with the chemical potential shift expected from electron doping. However, the new structure at E_F extends to 1.5 eV, contradicting a previous study that reported the shape of the valence and conduction band is similar to that of TiNCl [3]. It is difficult to explain the observed

valence band structure of Na_xTiNCl, especially the spectral structure near E_F, only by the rigid band shift of that of TiNCl.

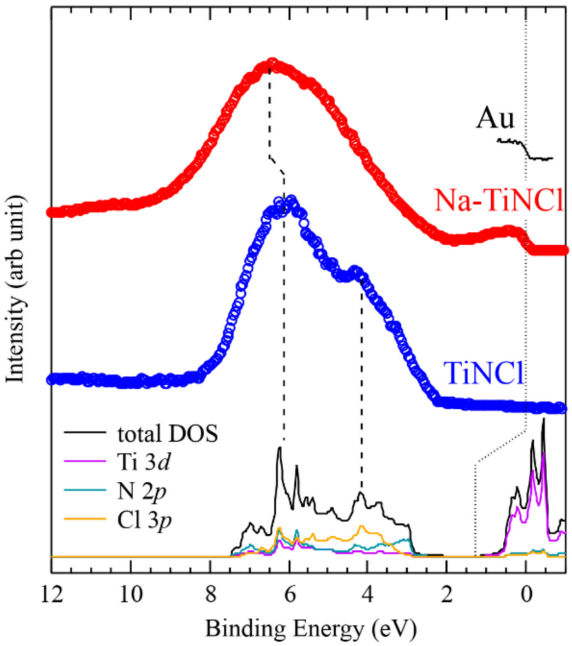

Figure 3. Valence band photoemission spectra of TiNCl (blue open circles) and Na_xTiNCl (red open circles), together with calculated total and partial DOS of TiNCl. E_F of the calculation is set to the conduction band's bottom and shifted to 1.3 eV toward the higher binding energy side. Reproduced with permission from Reference [30]. © (2019) The Physical Society of Japan.

An electronic band for the appearance of superconductivity is still unclear in this material. We have to wait for the result of ARPES to clarify it, but at present, the presence of the fine structure required to exhibit superconductivity has been suggested from a PES study using hard X-ray [58]. TiNCl prepared by the above-mentioned synthetic route using $NaNH_2$ appeared highly electron-doped, albeit without superconductivity. As an investigation of the origin, it became clear that there is a slight difference in Ti 2*p*. In comparing the core-level spectrum of Ti 2*p* with Na-intercalated samples, a fine structure around 455.5 eV emerges other than the shoulder-like component of the main structure of $Na_{0.1}TiNCl$. Although the area of the fine structure is small, peak fitting can be performed reliably, as shown in Figure 4 [58]. We can see a small contribution of component D in the peak fitting of $Na_{0.1}TiNCl$. However, it could not be observed in pristine non-superconducting samples even if it is in a highly electron-doped state. It did not appear unless the sample was Na-doped [58]. The difference in the preparation method changes the atmosphere during the synthesis. It may also change the hydrogen content of the resulting material. The electron doping in the TiNCl prepared by $NaNH_2$ may be attributed to the hydrogen content, affecting the oxidation state. Moreover, in the measurement of valence band spectra, the intensity of E_F and the area of component D in the doping dependence are correspondent. These findings suggest that even with the same electron doping, the electronic structure may change depending on the effective carrier insertion, determining whether or not superconductivity appears. Overall, component D seems to be a necessary structure for the appearance of superconductivity.

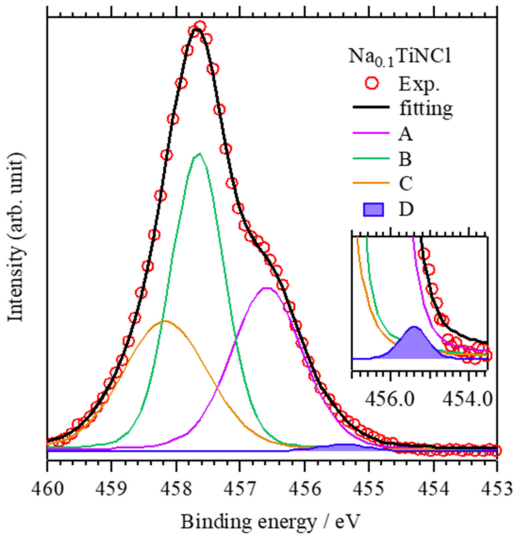

Figure 4. A result of peak fitting of Ti 2*p* hard X-ray PES spectra in $Na_{0.1}$TiNCl. The inset is an enlargement scale of component D. Although the area is small, it does not appear in non-superconducting TiNCl, even if it is highly electron-doped. Reprinted from Ref. [58].

3.2. Metalization of TiNCl Induced by Soft X-ray Irradiation

In the β-form *MNX*, the carrier control has also been performed by off stoichiometry or deintercalation of *X* [72]. Since TiNCl is easily thermally decomposed into TiN by annealing [49,54,73], such a carrier control is challenging, but irradiation of soft X-rays can achieve the metalization [74].

In the time courses of soft X-rays irradiation, the peak area of Ti^{4+} in the Ti 2*p* core-level spectrum decreased with the irradiation time, and the intensity of the shoulder structure also increased gradually (Figure 5). The intensity of the Cl 2*p* spectrum after the soft X-ray irradiation decreased gradually, which suggests the irradiation induces the desorption of Cl atoms from the surface [74]. As a result, a clear Fermi edge structure was observed in the valence band spectrum after 150 min irradiation suggesting the metallic nature of the measured region of the sample surface, as shown in Figure 5e [74].

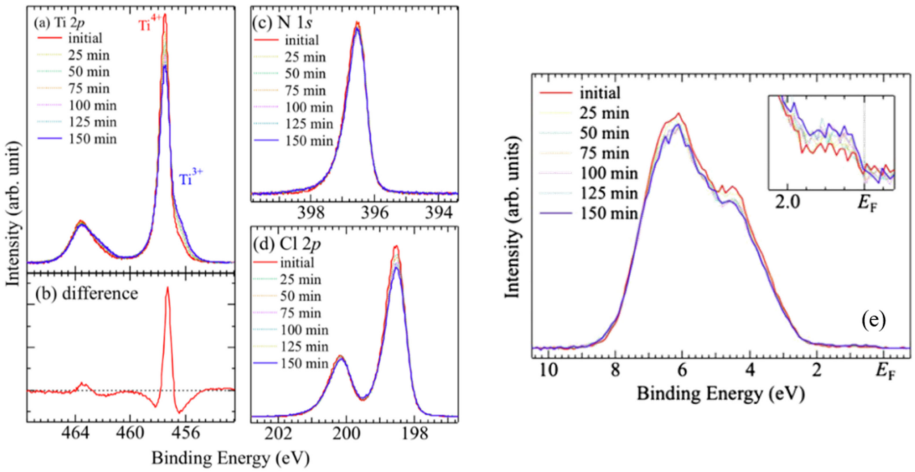

Figure 5. Soft X-ray irradiation time dependence of PES spectra. (**a**) Ti 2*p* core-level spectra irradiated from the initial to 150 min every 25 min. (**b**) Difference between the initial and 150 min of the spectra in (**a**). (**c**,**d**) are analogous spectra to (**a**) for the N 1*s* and Cl 2*p* core-level, respectively. (**e**) The valence band PES spectra. Inset shows the enlargement of the spectra near E_F. Reprinted with permission from Ref. [74]. Copyright 2022 IOP Publishing.

Figure 6 shows the temperature dependence of magnetic susceptibility of the pristine and irradiated samples. A weak diamagnetic signal was observed around 2 K in the pristine sample. The signal is attributed to that from TiN appearing by decomposition of TiNCl. Apart from the TiN, we can see that the other small diamagnetization near 14 K in the sample irradiated with soft X-rays for 30 min in the beam diameter region of ~20 μm (denoted as A). The signal becomes large when the area is expanded to about 0.5 × 0.5 mm^2 by repeating irradiation for 3 min (denoted as B). When the decomposition of TiNCl is promoted by the irradiation, the TiN content increases, which appears as a two-step transition resulting in the enhancement of the total VF.

On the other hand, it should be noted that the VF at 5 K, which is above the T_c of TiN, becomes several times larger, as shown in the inset of Figure 6. These facts suggest that the surface region irradiated with soft X-rays is electron-doped by Cl deintercalation and becomes metallic and superconducting. This technique is significant because it enables carrier control by deintercalation in α-form, which was not achieved with conventional synthetic methods. It can be expected to further the exploration of new functionality in α-form.

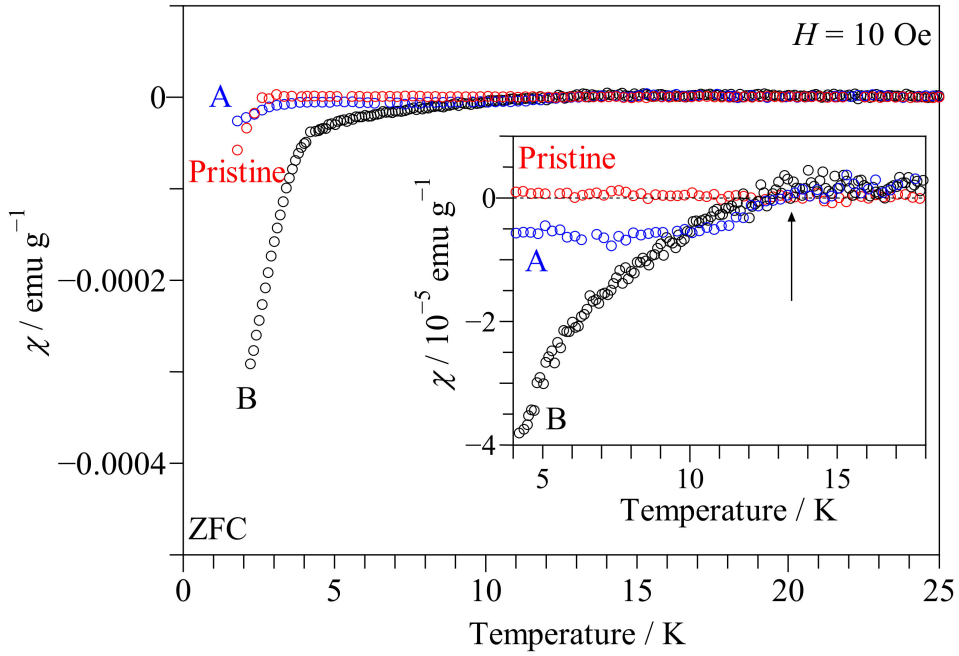

Figure 6. Temperature dependence of magnetic susceptibility in the zero-field-cooling mode of pristine TiNCl compared with soft X-ray irradiated samples. The irradiation conditions are: (**A**) 30 min in beam spot area, (**B**) 0.5 × 0.5 mm^2 by repeating 3 min irradiation. The pristine sample did not show any specific magnetic behavior except for a tiny contribution of TiN below 5 K. The irradiated samples showed a weak diamagnetic signal around 14 K. The inset shows the enlargement scale.

4. Conclusions

More than ten years have passed since discovering superconductivity in TiNCl in 2009. However, experimental research on α-form compounds has only just begun, despite the expectation of fantastic functionality utilizing two-dimensionality. We have developed synthetic methods in recent years, and the research has started reigniting. Spectroscopic measurements have gradually become possible even for α-form intercalated superconducting samples, which are far more moisture sensitive than β-form compounds. This progress has revealed that there are still unquantified questions such as the amount of hydrogen content for the superconducting properties. Observations of band dispersion by ARPES with further technological innovation would elucidate the whole picture of exotic superconductivity by comparing the electronic structure for both α- and β-forms

with different *M*-N layers. Further development of synthetic methods, including the carrier control by X-ray irradiation, may also be expected to acquire new functionality utilizing the two-dimensionality of TiNCl.

Funding: This research was funded by the Japan Society for the Promotion of Science (JSPS) through JSPS KAKENHI Grant Number JP18K04707, JP18KK0076 and 22K05289.

Data Availability Statement: The data that support the findings of this study are available from the corresponding author upon reasonable request.

Acknowledgments: The authors express their immeasurable gratitude to Emeritus Professor Shoji Yamanaka of Hiroshima University for his helpful suggestions throughout this study. The main results on TiNCl presented in this article were partly supported by the Japan Society for the Promotion of Science (JSPS) through JSPS KAKENHI Grant Number JP18K04707 and Promotion of Joint International Research (B) (JP18KK0076) from the Ministry of Education, Culture, Sports, Science and Technology of Japan (MEXT). The photoemission studies were performed at Spring-8 BL25SU under proposal numbers 2019B1454 and 2020A1670. Preliminary studies on soft X-ray irradiation-induced superconductivity were performed at BL5, HiSOR.

Conflicts of Interest: The authors declare no conflict of interest.

References

1. Yamanaka, S.; Kawaji, H.; Hotehama, K.; Ohashi, M. A new layer-structured nitride superconductor. Lithium-intercalated β-zirconium nitride chloride, Li_xZrNCl. *Adv. Mater.* **1996**, *8*, 771–774. [CrossRef]
2. Yamanaka, S.; Hotehama, K.I.; Kawaji, H. Superconductivity at 25.5K in electron-doped layered hafnium nitride. *Nature* **1998**, *392*, 580–582. [CrossRef]
3. Yamanaka, S.; Yasunaga, T.; Yamaguchi, K.; Tagawa, M. Structure and superconductivity of the intercalation compounds of TiNCl with pyridine and alkali metals as intercalants. *J. Mater. Chem.* **2009**, *19*, 2573. [CrossRef]
4. Yamanaka, S. Intercalation and superconductivity in ternary layer structured metal nitride halides (*MNX*: *M* = Ti, Zr, Hf; *X* = Cl, Br, I). *J. Mater. Chem.* **2010**, *20*, 2922–2933. [CrossRef]
5. Juza, R.; Heners, J. Über Nitridhalogenide des Titans und Zirkons. *Z. Für Anorg. Und Allg. Chem.* **1964**, *332*, 159–172. [CrossRef]
6. Zhang, S.; Tanaka, M.; Zhu, H.; Yamanaka, S. Superconductivity of layered β-HfNCl with varying electron-doping concentrations and interlayer spacings. *Supercond. Sci. Technol.* **2013**, *26*, 085015. [CrossRef]
7. Ueno, K.; Shimotani, H.; Yuan, H.; Ye, J.; Kawasaki, M.; Iwasa, Y. Field-induced superconductivity in electric double layer transistors. *J. Phys. Soc. Jpn.* **2014**, *83*, 032001. [CrossRef]
8. Saito, Y.; Kasahara, Y.; Ye, J.; Iwasa, Y.; Nojima, T. Metallic ground state in an ion-gated two-dimensional superconductor. *Science* **2015**, *350*, 409–413. [CrossRef]
9. Zhang, S.; Gao, M.-R.; Fu, H.-Y.; Wang, X.-M.; Ren, Z.-A.; Chen, G.-F. Electric Field Induced Permanent Superconductivity in Layered Metal Nitride Chlorides HfNCl and ZrNCl. *Chin. Phys. Lett.* **2018**, *35*, 097401. [CrossRef]
10. Wang, X.; Zhang, S.; Fu, H.; Gao, M.; Ren, Z.; Chen, G. Dominant role of processing temperature in electric field induced superconductivity in layered ZrNBr. *N. J. Phys.* **2019**, *21*, 023002. [CrossRef]
11. Nakagawa, Y.; Kasahara, Y.; Nomoto, T.; Arita, R.; Nojima, T.; Iwasa, Y. Gate-controlled BCS-BEC crossover in a two-dimensional superconductor. *Science* **2021**, *372*, 190–195. [CrossRef] [PubMed]
12. Nakagawa, Y.; Saito, Y.; Nojima, T.; Inumaru, K.; Yamanaka, S.; Kasahara, Y.; Iwasa, Y. Gate-controlled low carrier density superconductors: Toward the two-dimensional BCS-BEC crossover. *Phys. Rev. B* **2018**, *98*, 064512. [CrossRef]
13. Taguchi, Y.; Kitora, A.; Iwasa, Y. Increase in Tc upon reduction of doping in Li_xZrNCl superconductors. *Phys. Rev. Lett.* **2006**, *97*, 107001. [CrossRef] [PubMed]
14. Peng, J.; Zhang, S. Synthesis and Superconductivity of Electron-Doped β-ZrNCl with Partial Substitution of Ti on Zr Site. *J. Supercond. Nov. Magn.* **2018**, *31*, 61–65. [CrossRef]
15. Tou, H.; Maniwa, Y.; Koiwasaki, T.; Yamanaka, S. Unconventional superconductivity in electron-doped layered $Li_{0.48}(THF)_yHfNCl$. *Phys. Rev. Lett.* **2001**, *86*, 5775–5778. [CrossRef]
16. Taguchi, Y.; Hisakabe, M.; Iwasa, Y. Specific heat measurement of the layered nitride superconductor Li_xZrNCl. *Phys. Rev. Lett.* **2005**, *94*, 2–5. [CrossRef]
17. Yokoya, T.; Ishiwata, Y.; Shin, S.; Shamoto, S.; Iizawa, K.; Kajitani, T.; Hase, I.; Takahashi, T. Changes of electronic structure across the insulator-to-metal transition of quasi-two-dimensional Na-intercalated β-HfNCl studied by photoemission and X-ray absorption. *Phys. Rev. B* **2001**, *64*, 153107. [CrossRef]

18. Takeuchi, T.; Tsuda, S.; Yokoya, T.; Tsukamoto, T.; Shin, S.; Hirai, A.; Shamoto, S.; Kajitani, T. Soft X-ray emission and high-resolution photoemission study of quasi-two-dimensional superconductor Na_xHfNCl. *Physica C* **2003**, *392–396*, 127–129. [CrossRef]
19. Yokoya, T.; Takeuchi, T.; Tsuda, S.; Kiss, T.; Higuchi, T.; Shin, S.; Iizawa, K.; Shamoto, S.; Kajitani, T.; Takahashi, T. Valence-band photoemission study of β-ZrNCl and the quasi-two-dimensional superconductor Na_xZrNCl. *Phys. Rev. B* **2004**, *70*, 193103. [CrossRef]
20. Tou, H.; Maniwa, Y.; Yamanaka, S. Superconducting characteristics in electron-doped layered hafnium nitride: ^{15}N isotope effect studies. *Phys. Rev. B* **2003**, *67*, 100509. [CrossRef]
21. Weht, R.; Filippetti, A.; Pickett, W.E. Electron doping in the honeycomb bilayer superconductors (Zr, Hf)NCl. *Europhys. Lett.* **1999**, *48*, 320–325. [CrossRef]
22. Sugimoto, A.; Sakai, Y.; Ekino, T.; Zhang, S.; Tanaka, M.; Yamanaka, S.; Gabovich, A.M. Scanning Tunnelling Microscopy and Spectroscopy of the Layered Nitride Superconductor α-Na_xTiNCl. *Phys. Procedia* **2016**, *81*, 73–76. [CrossRef]
23. Ekino, T.; Takasaki, T.; Muranaka, T.; Fujii, H.; Akimitsu, J.; Yamanaka, S. Tunneling spectroscopy of MgB_2 and $Li_{0.5}(THF)_yHfNCl$. *Phys. B Condens. Matter* **2003**, *328*, 23–25. [CrossRef]
24. Kawaji, H.; Hotehama, K.I.; Yamanaka, S. Superconductivity of Alkali Metal Intercalated β-Zirconium Nitride Chloride, A_xZrNCl (A = Li, Na, K). *Chem. Mater.* **1997**, *9*, 2127–2130. [CrossRef]
25. Takano, T.; Kishiume, T.; Taguchi, Y.; Iwasa, Y. Interlayer-spacing dependence of T_c in Li_xM_yHfNCl (M: Molecule) superconductors. *Phys. Rev. Lett.* **2008**, *100*, 247005. [CrossRef]
26. Kasahara, Y.; Kishiume, T.; Kobayashi, K.; Taguchi, Y.; Iwasa, Y. Superconductivity in molecule-intercalated Li_xZrNCl with variable interlayer spacing. *Phys. Rev. B* **2010**, *82*, 054504. [CrossRef]
27. Kasahara, Y.; Kishiume, T.; Takano, T.; Kobayashi, K.; Matsuoka, E.; Onodera, H.; Kuroki, K.; Taguchi, Y.; Iwasa, Y. Enhancement of Pairing Interaction and Magnetic Fluctuations toward a Band Insulator in an Electron-Doped Li_xZrNCl Superconductor. *Phys. Rev. Lett.* **2009**, *103*, 077004. [CrossRef]
28. Kotegawa, H.; Oshiro, S.; Shimizu, Y.; Tou, H.; Kasahara, Y.; Kishiume, T.; Taguchi, Y.; Iwasa, Y. Strong suppression of coherence effect and appearance of pseudogap in the layered nitride superconductor Li_xZrNCl: ^{91}Zr- and ^{15}N-NMR studies. *Phys. Rev. B* **2014**, *90*, 020503. [CrossRef]
29. Kasahara, Y.; Kuroki, K.; Yamanaka, S.; Taguchi, Y. Unconventional superconductivity in electron-doped layered metal nitride halides MNX (M = Ti, Zr, Hf; X = Cl, Br, I). *Physica C* **2015**, *514*, 354–367. [CrossRef]
30. Kataoka, N.; Terashima, K.; Tanaka, M.; Hosoda, W.; Taniguchi, T.; Wakita, T.; Muraoka, Y.; Yokoya, T. μ-PES Studies on TiNCl and Quasi-two-dimensional Superconductor Na-intercalated TiNCl. *J. Phys. Soc. Jpn.* **2019**, *88*, 104709. [CrossRef]
31. Yamanaka, S.; Umemoto, K.; Zheng, Z.; Suzuki, Y.; Matsui, H.; Toyota, N.; Inumaru, K. Preparation and superconductivity of intercalation compounds of TiNCl with aliphatic amines. *J. Mater. Chem.* **2012**, *22*, 10752–10762. [CrossRef]
32. Zhang, S.; Tanaka, M.; Yamanaka, S. Superconductivity in electron-doped layered TiNCl with variable interlayer coupling. *Phys. Rev. B* **2012**, *86*, 024516. [CrossRef]
33. Liang, Y.; Dai, Y.; Ma, Y.; Ju, L.; Wei, W.; Huang, B. Novel titanium nitride halide TiNX (X = F, Cl, Br) monolayers: Potential materials for highly efficient excitonic solar cells. *J. Mater. Chem. A* **2018**, *6*, 2073–2080. [CrossRef]
34. Liu, J.; Li, X.-B.; Wang, D.; Liu, H.; Peng, P.; Liu, L.-M. Single-layer Group-IVB nitride halides as promising photocatalysts. *J. Mater. Chem. A* **2014**, *2*, 6755. [CrossRef]
35. Zhou, L.; Zhuo, Z.; Kou, L.; Du, A.; Tretiak, S. Computational Dissection of Two-Dimensional Rectangular Titanium Mononitride TiN: Auxetics and Promises for Photocatalysis. *Nano Lett.* **2017**, *17*, 4466–4472. [CrossRef]
36. Zhang, X.; Zhang, Z.; Zhao, X.; Wu, D.; Zhang, X.; Zhou, Z. Tetragonal-structured anisotropic 2D metal nitride monolayers and their halides with versatile promises in energy storage and conversion. *J. Mater. Chem. A* **2017**, *5*, 2870–2875. [CrossRef]
37. Wang, A.; Wang, Z.; Du, A.; Zhao, M. Band inversion and topological aspects in a TiNI monolayer. *Phys. Chem. Chem. Phys.* **2016**, *18*, 22154–22159. [CrossRef]
38. Zhang, Z.; Zhang, R.-W.; Li, X.; Koepernik, K.; Yao, Y.; Zhang, H. High-Throughput Screening and Automated Processing toward Novel Topological Insulators. *J. Phys. Chem. Lett.* **2018**, *9*, 6224–6231. [CrossRef]
39. Li, X.; Zhang, Z.; Yao, Y.; Zhang, H. High throughput screening for two-dimensional topological insulators. *2D Mater.* **2018**, *5*, 045023. [CrossRef]
40. Rostami Osanloo, M.; Saadat, A.; Van de Put, M.L.; Laturia, A.; Vandenberghe, W.G. Transition-metal nitride halide dielectrics for transition-metal dichalcogenide transistors. *Nanoscale* **2022**, *14*, 157–165. [CrossRef]
41. Hossain, M.M.; Naqib, S.H. Structural, elastic, electronic, andoptical properties of layered TiNX (X = F, Cl, Br, I) compounds: A density functional theory study. *Mol. Phys.* **2020**, *118*, e1609706. [CrossRef]
42. Guo, Y.; Peng, J.; Qin, W.; Zeng, J.; Zhao, J.; Wu, J.; Chu, W.; Wang, L.; Wu, C.; Xie, Y. Freestanding Cubic ZrN Single-Crystalline Films with Two-Dimensional Superconductivity. *J. Am. Chem. Soc.* **2019**, *141*, 10183–10187. [CrossRef] [PubMed]
43. Schurz, C.M.; Shlyk, L.; Schleid, T.; Niewa, R. Superconducting nitride halides MNX (M = Ti, Zr, Hf; X = Cl, Br, I). *Z. Krist.* **2011**, *226*, 395–416. [CrossRef]
44. Juza, R.; Klose, W. Die Kristallstruktur des Zirkonnitridjodids. *Angew. Chem.* **1959**, *71*, 161. [CrossRef]

45. Juza, R.; Friedrichsen, H. Die Kristallstruktur von β-ZrNCl und β-ZrNBr. *Z. Anorg. Allg. Chem.* **1964**, *332*, 173–178. [CrossRef]
46. Juza, R.; Klose, W. Über ein Nitridjodid des Zirkons. *Z. Anorg. Allg. Chem. Anorg. Allg. Chem.* **1964**, *327*, 207–214. [CrossRef]
47. Cross, J.B.; Schlegel, H.B. Molecular orbital studies of titanium nitride chemical vapor deposition: Gas phase β -elimination. *Chem. Phys. Lett.* **2001**, *340*, 343–347. [CrossRef]
48. Umanskii, S.Y.; Novoselov, K.P.; Minushev, A.K.; Siodmiak, M.; Frenking, G.; Korkin, A.A. Thermodynamics and kinetics of initial gas phase reactions in chemical vapor deposition of titanium nitride. Theoretical study of $TiCl_4$ ammonolysis. *J. Comput. Chem.* **2001**, *22*, 1366–1376. [CrossRef]
49. Saeki, Y.; Matsuzaki, R.; Yajima, A.; Akiyama, M. Reaction Process of Titanium Tetrachloride with Ammonia in the Vapor Phase and Properties of the Titanium Nitride Formed. *Bull. Chem. Soc. Jpn.* **1982**, *55*, 3193–3196. [CrossRef]
50. Fowles, G.W.A.; Pollard, F.H. Studies on the behaviour of halides of the transition metals with ammonia. Part II. The reaction of titanium tetrachloride with ammonia. *J. Chem. Soc.* **1953**, *22*, 2588. [CrossRef]
51. Kurtz, S.R.; Gordon, R.G. Chemical vapor deposition of titanium nitride at low temperatures. *Thin Solid Films* **1986**, *140*, 277–290. [CrossRef]
52. Ohashi, M.; Yamanaka, S.; Hattori, M. Chemical vapor transport of layer structured crystal β-ZrNCl. *J. Solid State Chem.* **1988**, *77*, 342–347. [CrossRef]
53. Yajima, A.; Segawa, Y.; Matsuzaki, R.; Saeki, Y. Reaction Process of Zirconium Tetrachloride with Ammonia in the Vapor Phase and Properties of the Zirconium Nitride Formed. *Bull. Chem. Soc. Jpn.* **1983**, *56*, 2638–2642. [CrossRef]
54. Sosnov, E.A.; Malkov, A.A.; Malygin, A.A. Chemical transformations at the silica surface upon sequential interactions with titanium tetrachloride and ammonia vapors. *Russ. J. Gen. Chem.* **2015**, *85*, 2533–2540. [CrossRef]
55. Ohashi, M.; Yamanaka, S.; Hattori, M. Synthesis of β-ZrClN by Thermal Decomposition of Zirconium(IV) Amide Trichloride. *Bull. Chem. Soc. Jpn.* **1986**, *59*, 2627–2628. [CrossRef]
56. Odahara, J.; Sun, W.; Miura, A.; Rosero-Navarro, N.C.; Nagao, M.; Tanaka, I.; Ceder, G.; Tadanaga, K. Self-Combustion Synthesis of Novel Metastable Ternary Molybdenum Nitrides. *ACS Mater. Lett.* **2019**, *1*, 64–70. [CrossRef]
57. Miura, A. Low-temperature synthesis and rational design of nitrides and oxynitrides for novel functional material development. *J. Ceram. Soc. Jpn.* **2017**, *125*, 552–558. [CrossRef]
58. Tanaka, M.; Kataoka, N.; Matsumoto, R.; Inumaru, K.; Takano, Y.; Yokoya, T. Synthetic Route of Layered Titanium Nitride Chloride TiNCl Using Sodium Amide. *ACS Omega* **2022**, *7*, 6375–6380. [CrossRef]
59. Kuhn, A.; Hoppe, H.; Strähle, J.; Garcia-Alvarado, F. Electrochemical Lithium Intercalation in Titanium Nitride Chloride. *J. Electrochem. Soc.* **2004**, *151*, A843. [CrossRef]
60. Ohashi, M.; Uyeoka, K.; Yamanaka, S.; Hattori, M. Co-Intercalation of Tetrahydrofuran and Propylene Carbonate with Alkali Metals in β-ZrNCl Layer Structured Crystal. *Bull. Chem. Soc. Jpn.* **1991**, *64*, 2814–2818. [CrossRef]
61. Zhang, S.; Tanaka, M.; Watanabe, E.; Zhu, H.; Inumaru, K.; Yamanaka, S. Superconductivity of alkali metal intercalated TiNBr with alpha-type nitride layers. *Supercond. Sci. Technol.* **2013**, *26*, 122001. [CrossRef]
62. Yamanaka, S.; Okumura, H.; Zhu, L. Alkali metal intercalation in layer structured α-HfNBr. *J. Phys. Chem. Solids* **2004**, *65*, 565–569. [CrossRef]
63. Hotehama, K.; Koiwasaki, T.; Umemoto, K.; Yamanaka, S.; Tou, H. Effect of Swelling on the Superconducting Characteristics in Electron-Doped β-ZrNCl and HfNCl. *J. Phys. Soc. Jpn.* **2010**, *79*, 014707. [CrossRef]
64. Harshman, D.R.; Fiory, A.T. Modeling Intercalated Group-4-Metal Nitride Halide Superconductivity with Interlayer Coulomb Coupling. *J. Supercond. Nov. Magn.* **2015**, *28*, 2967–2978. [CrossRef]
65. Yin, Q.; Ylvisaker, E.R.; Pickett, W.E. Spin and charge fluctuations in α-structure layered nitride superconductors. *Phys. Rev. B* **2011**, *83*, 014509. [CrossRef]
66. Felser, C.; Seshadri, R. Electronic structures and instabilities of ZrNCl and HfNCl: Implications for superconductivity in the doped compounds. *J. Mater. Chem.* **1999**, *9*, 459–464. [CrossRef]
67. Kuroki, K. Spin-fluctuation-mediated *d+id'* pairing mechanism in doped β-*M*NCl (*M*=Hf, Zr) superconductors. *Phys. Rev. B* **2010**, *81*, 104502. [CrossRef]
68. Kusakabe, K. Pair-hopping mechanism of superconductivity activated by the nano-space layered structure. *J. Phys. Chem. Solids* **2012**, *73*, 1546–1549. [CrossRef]
69. Yin, Z.P.; Kutepov, A.; Kotliar, G. Correlation-Enhanced Electron-Phonon Coupling: Applications of GW and Screened Hybrid Functional to Bismuthates, Chloronitrides, and Other High-T_c Superconductors. *Phys. Rev. X* **2013**, *3*, 021011. [CrossRef]
70. Sugimoto, A.; Shohara, K.; Ekino, T.; Zheng, Z.; Yamanaka, S. Nanoscale electronic structure of the layered nitride superconductors α-K_xTiNCl and β-HfNCl y observed by scanning tunneling microscopy and spectroscopy. *Phys. Rev. B* **2012**, *85*, 144517. [CrossRef]
71. Ino, A.; Yamazaki, K.; Yamasaki, T.; Higashiguchi, M.; Shimada, K.; Namatame, H.; Taniguchi, M.; Oguchi, T.; Chen, X.; Yamanaka, S. Angle-resolved-photoemission study of layer-structured nitride β-HfNCl. *J. Electron Spectros. Relat. Phenom.* **2005**, *144–147*, 667–669. [CrossRef]
72. Zhu, L.; Ohashi, M.; Yamanaka, S. Zirconium nitride derived from layer-structured β-ZrNCl by deintercalation of chlorine layers. *Chem. Mater.* **2002**, *14*, 4517–4521. [CrossRef]

73. Hegde, R.I.; Fiordalice, R.W.; Tobin, P.J. TiNCl formation during low-temperature, low-pressure chemical vapor deposition of TiN. *Appl. Phys. Lett.* **1993**, *62*, 2326–2328. [CrossRef]
74. Kataoka, N.; Tanaka, M.; Hosoda, W.; Taniguchi, T.; Fujimori, S.; Wakita, T.; Muraoka, Y.; Yokoya, T. Soft X-ray irradiation induced metallization of layered TiNCl. *J. Phys. Condens. Matter* **2021**, *33*, 035501. [CrossRef]